

Overcoming the entanglement barrier in quantum many-body dynamics via space-time duality

Alessio Lerose,¹ Michael Sonner,¹ and Dmitry A. Abanin¹

¹*Department of Theoretical Physics, University of Geneva,
Quai Ernest-Ansermet 30, 1205 Geneva, Switzerland*

Describing non-equilibrium properties of quantum many-body systems is challenging due to high entanglement in the wavefunction. We take an open-quantum-system viewpoint and describe evolution of local observables in terms of the influence matrix (IM), which encodes the effects of a many-body system as an environment for a local subsystem. Recent works found that in many dynamical regimes the IM of an infinite system has low *temporal entanglement* and can be efficiently represented as a matrix-product state (MPS). Yet, direct iterative constructions of the IM encounter highly entangled intermediate states – a temporal entanglement barrier (TEB). We argue that TEB is ubiquitous, and elucidate its physical origin via a semiclassical quasiparticle picture that captures the exact behavior of integrable spin chains. Further, we show that a TEB also arises in chaotic spin chains, which lack well-defined quasiparticles. Based on these insights, we formulate an alternative *light-cone growth* algorithm, which provably avoids TEB, thus providing an efficient construction of the thermodynamic-limit IM as a MPS. This work demonstrates the efficiency of the IM approach to studying thermalization and transport in strongly interacting quantum systems.

A central task of many-body physics is understanding how macroscopic laws emerge from microscopic dynamics. Describing quantum many-body dynamics is especially challenging, as the exponential complexity of general many-body wavefunctions $|\Psi\rangle$ limits the reach of numerical simulations. While area-law entangled ground states can be compactly represented using tensor networks [1], out-of-equilibrium states $|\Psi(t)\rangle$ typically exhibit large quantum entanglement [2–4], which precludes their efficient parametrization. This poses fundamental challenges for the computation of properties such as transport character and coefficients.

The difficulty of accessing the late-time hydrodynamic regime appears somewhat paradoxical, as in this regime local subsystems are in near-equilibrium states. The complex non-local correlations that make $|\Psi(t)\rangle$ intractable are expected to enter the hydrodynamic description indirectly, by building thermodynamic entropy of local subsystems. It is thus conceivable that one may efficiently describe the emergence of hydrodynamic behavior from the evolution of simple initial states by systematically converting the “irrelevant” parts of quantum entanglement into classical-statistical entropy.

Several approaches have been recently proposed to capture quantum many-body dynamics beyond the entanglement wall [5–13]. Their common strategy is to modify the time-evolution update rule of the relevant object (many-body wavefunction [5, 6, 10], density matrix [7–9, 12, 13], Heisenberg-picture observable [11]) by introducing a truncation or damping scheme for non-local quantum information, but aiming to preserve local correlations. While remark-

able success has been reported in describing diffusion in certain quantum spin chains, the general applicability of these approaches remains unclear.

In this work, we follow a conceptually different route to describe dynamics of local observables in a finite subsystem \mathcal{S} . Working with the *instantaneous* quantum state of the full system (e.g., of $|\Psi(t)\rangle$) can be disadvantageous, since it is difficult to discern the correlations within \mathcal{S} and its complement \mathcal{E} which do affect the later evolution of \mathcal{S} , from those which do not. Inspired by the framework of open quantum systems, we encode the dynamical influence of \mathcal{E} on \mathcal{S} as a systematically compressed effective environment, with both memory and dissipation. Our central tool is the Feynman-Vernon influence functional, introduced to describe a quantum particle interacting with a bath of harmonic oscillators [14, 15]. Based on this, we formulated the influence matrix (IM) approach to study dynamics in quantum circuits [16, 17] (see also [18, 19]). Recent insights on the IM structure of generic [16, 20] and solvable [21–25] models suggest that this approach can be efficient in regimes inaccessible to other methods.

Despite its promise, the general efficiency of the IM approach remains to be understood. In particular, Refs. [17, 20] observed that constructing the IM of an infinite system by gradually including more degrees of freedom into \mathcal{E} leads to a temporal entanglement barrier (TEB): the IM viewed as a fictitious wavefunction in the time domain becomes highly entangled in intermediate steps. Thus, TEB poses a challenge for reliable computation of the IM of an infinite chain, even when it has low entanglement.

Here, we investigate the origin of TEB and the

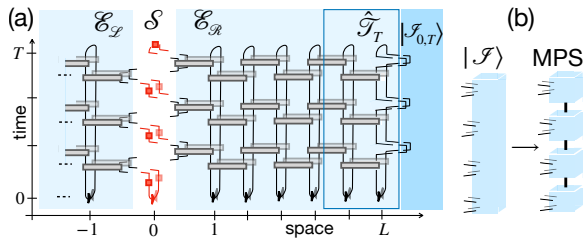


Figure 1. (a): IM approach for a quantum spin chain. Evolution of “ket” and “bra” components of the initial density matrix (here factorized, black) is generated by two conjugated unitary circuits (forward and backward sheets of gray “bricks”). Red squares denote operators acting only on \mathcal{S} (here a single spin). Their time-ordered correlators are influenced by the spins in the left and right complements $\mathcal{E}_{\mathcal{L}}, \mathcal{E}_{\mathcal{R}}$ of \mathcal{S} , traced out at final time T . The blue-shaded tensors are the two associated IMs. The OBC IM $|\mathcal{I}_{0,T}\rangle$ and the dual transfer matrix $\hat{\mathcal{T}}_T$ are highlighted. (b): MPS representation of an IM.

efficiency of the IM approach. We argue that an extensive TEB generally arises from the backflow of quantum information from a finite \mathcal{E} back to \mathcal{S} . We analyze a solvable model where quantum information is carried by stable ballistic quasiparticles and quantify the TEB effect in terms of their properties. We further show that TEB is not limited to such models, and also occurs in chaotic quantum many-body dynamics. This finding suggests an alternative construction algorithm, which we dub *light-cone growth algorithm* (LCGA). We implement it within the framework of matrix-product states (MPSs), and give a proof that it circumvents TEB.

Influence matrix approach. We consider spin-1/2 chains initialized in a factorized state, and take \mathcal{S} as a finite interval. Within the IM approach, the degrees of freedom in the complement \mathcal{E} are traced out, leaving an effective open-quantum-system evolution for \mathcal{S} . The influence of \mathcal{E} on \mathcal{S} is encoded in non-local-in-time “self-interactions” of \mathcal{S} [14]. Concretely, we express dynamics of \mathcal{S} via a Keldysh path integral over trajectories of spins in \mathcal{S} and \mathcal{E} . Path integration over the latter results in a functional \mathcal{I} of the trajectory of \mathcal{S} . This can be obtained by representing time-evolution as a unitary circuit [26], and viewing the IM as the contraction of the associated tensor network [blue shaded in Fig. 1(a)] [16].

The IM can be viewed as a fictitious one-dimensional wavefunction on the Schwinger-Keldysh contour $|\mathcal{I}\rangle$ and thus compressed as MPS [Fig. 1(b)] [16, 20]. The χ -dimensional virtual space associated with the MPS bonds may be physically interpreted as the density-matrix space of an effective dissipative $\sqrt{\chi}$ -dimensional environment $\tilde{\mathcal{E}}$ pro-

ducing nearly identical influence on \mathcal{S} as that of \mathcal{E} . The compression from \mathcal{E} to $\tilde{\mathcal{E}}$ is made possible by allowing Markovian dissipation in the effective open-quantum-system problem [27]. The dissipation acting at time $t \in [0, T]$ erases the quantum information that flows away at t without ever coming back to \mathcal{S} before T . Importantly, in this approach one does not need to artificially decide which part of quantum information gets truncated at intermediate time t : The compression algorithm systematically does it by exploiting *global* knowledge of the process in the whole time interval $[0, T]$.

The IM \mathcal{I} contains exactly the *minimum* amount of information pertaining to \mathcal{E} necessary to access arbitrary temporal correlations in \mathcal{S} . The complexity of this object is tied to the extent of such temporal correlations. We quantify this complexity via the *temporal entanglement* (TE) entropy [16, 18] of $|\mathcal{I}\rangle$. Since fast relaxation to equilibrium is associated with fast decay of temporal correlations, TE is expected to scale favorably with evolution time in thermalizing systems, suggesting an efficient MPS representation [16]. While quantitative predictions of TE scaling for general systems are currently lacking, a slow sublinear scaling of TE with evolution time has been shown numerically and analytically in several cases [17, 21–25, 28].

Temporal entanglement barrier. Previous works [16–18, 20] found the IM of an infinite chain by repeatedly applying a dual transfer matrix $\hat{\mathcal{T}}$, acting along the spatial direction, to some initial vector. Making reference to Fig. 1(a), we consider the IM $|\mathcal{I}_{L,T}\rangle$ of the right environment $\mathcal{E}_{\mathcal{R}}$ ($\equiv \mathcal{E}$ henceforth), consisting of L spins, for evolution time T . $\hat{\mathcal{T}}_T$ acts from right to left, including two extra sites in the environment at each application. The $L/2$ iterations of $\hat{\mathcal{T}}_T$ start from a boundary IM $|\mathcal{I}_{0,T}\rangle$. In Fig. 1(a), $|\mathcal{I}_{0,T}\rangle$ is the IM of an empty environment due to open boundary conditions (OBC) – a product of Bell pairs. As $|\mathcal{I}_{\ell,T}\rangle = \hat{\mathcal{T}}_T^{\ell/2} |\mathcal{I}_{0,T}\rangle$ “evolves” in space, its forward and backward parts [29] only get coupled at the boundaries $\tau = 0, T$: the latter corresponds to the final trace over \mathcal{E} , while the former is set by the choice of initial state $\rho_{\mathcal{E}}(0)$. Due to the strict light cone, iterations converge to the infinite-system IM $|\mathcal{I}_{\infty,T}\rangle$ for $L \geq v_{\max} t$, where v_{\max} is the Lieb-Robinson velocity [30] of the model, regardless of the choice of $|\mathcal{I}_{0,T}\rangle$.

References [17, 20] observed that the TE of intermediate IMs $|\mathcal{I}_{\ell,T}\rangle$ is non-monotonic in ℓ , reaching values much higher than that of $|\mathcal{I}_{\infty,T}\rangle$ – the behavior that we refer to as TEB. Intuitively, TEB can be traced back to the fact that $\hat{\mathcal{T}}_T^{\ell/2}$ enables one to compute correlations of the form $\langle \Psi(T) | \mathcal{O}_A \mathcal{O}_B | \Psi(T) \rangle$,

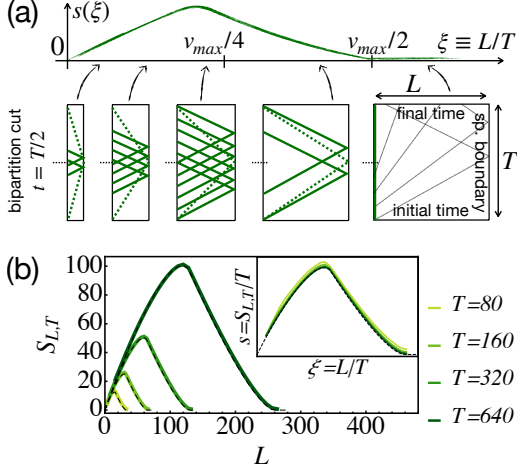


Figure 2. (a): Quasiparticle picture of TE scaling. Sketches in the bottom row: for IMs of right-environment with increasing size from left to right, dashed (solid) lines denote the trajectories of slowest (fastest) quasiparticles creating correlations across the IM cut. Top graph: resulting characteristic TEB shape. (b): Exact TEB of the OBC, infinite-temperature KIC for $g = \pi/4$, $J = 0.6\pi/4$. Dashed curves are the predictions of Eq. (1) with $w \equiv 0.93 \log 2$ (essentially superimposed). The left asymptote is a straight line $\lim_{T \rightarrow \infty} S_{L,T} = v_{TE} L$. The right asymptote $S_\infty = \lim_{T \rightarrow \infty} \lim_{L \rightarrow \infty} S_{L,T}$ is a small finite quantity [21].

where $\mathcal{O}_A, \mathcal{O}_B$ are arbitrary local operators supported in regions A and B separated by ℓ sites. Thus, one may expect the complexity of intermediate IMs, obtained via powers of \tilde{T}_T , to be similar to that of computing *non-local* correlations in $|\Psi(T)\rangle$, which, presumably, scales exponentially with T .

To better elucidate the physical origin of TEB, we consider a model with stable ballistic quasiparticles with maximum velocity v_{\max} . The dual evolution described above, with space and time interchanged, is particularly transparent when the dual circuit is unitary [31]. In this case, all quasiparticles move at the “speed of light” $v_{\max} = 2$, and one can adapt the Calabrese-Cardy picture of entanglement growth after a quantum quench [2]. For OBC, $|\mathcal{S}_{0,T}\rangle$ is a product state of $2T$ Bell pairs [see Fig. 1(a)], which

generates pairs of entangled quasiparticles spreading with opposite velocity. The bipartite entanglement of the final IM wave-function $|\mathcal{S}_{L,T}\rangle$ between intervals $[0, t]$ and $[t+1, T]$ can be computed quasiclassically by summing the contributions of pairs propagating to points across the cut. However, a novel aspect of our problem is given by the boundary conditions at $\tau = 0, T$. Their role is clearest in the original time-evolution perspective: a quasiparticle traveling with velocity v on the forward sheet until $\tau = T$ continues along a specular path on the backward sheet (cf. the “folding” arguments in Refs. [18, 19, 25]). Hence, returning to the dual evolution picture, each point of the $\tau = T$ boundary can be viewed as a source ($v > 0$) and sink ($v < 0$) of superimposed quasiparticle pairs propagating on the two sheets. For infinite-temperature initial state $\rho_{\mathcal{E}}(0) = \bigotimes_{j=1}^L \frac{1}{2}$, the $\tau = 0$ boundary plays the same role. Thus, these boundaries destroy the non-local correlations of the pairs generated by $|\mathcal{S}_{0,T}\rangle$, replacing them with local correlations between the forward and backward branch at equal time. As a result, when a quasiparticle hits a boundary (“absorption”), the corresponding initially entangled pair no longer contributes to TE, and has to be removed from the Calabrese-Cardy summation.

The generation of a counter-propagating entangled pair in the quasiparticle picture appears as *reflection* of an individual quasiparticle in the dual picture. Within the spatial evolution of $|\mathcal{S}\rangle$, pairs generated by a pure initial state $\rho_{\mathcal{E}}(0) = |\Psi_{\mathcal{E}}(0)\rangle\langle\Psi_{\mathcal{E}}(0)|$ at $\tau = 0$ [2] are interpreted as reflections of individual quasiparticles hitting the boundary [32]. Analogously, within the physical time evolution, pairs generated by the spatial boundary $|\mathcal{S}_{0,T}\rangle$ are interpreted as reflections of individual quasiparticles hitting the end of the chain and coming back to the subsystem \mathcal{S} . This elementary process leads to strong correlations between the remote past and future of \mathcal{S} , and hence to a sizeable TEB.

This picture is expected to hold for general models with stable quasiparticles, as illustrated in Fig. 2(a). We thus posit the following general formula for the leading behavior of TE entropy as $L \rightarrow \infty, T \rightarrow \infty$:

$$S_{L,T,t} = \int_0^t dt_{f,1} \int_t^T dt_{f,2} \int_0^T dt_i \int_{\omega_{\min}}^{\omega_{\max}} \frac{d\omega}{2\pi} w(\omega) \delta\left(t_{f,1} - t_i + \frac{L}{v(\omega)}\right) \delta\left(t_{f,2} - t_i - \frac{L}{v(\omega)}\right). \quad (1)$$

Here, t_i denotes the boundary point where a quasiparticle pair is created, $t_{f,1}, t_{f,2}$ are the arrival points, $[\omega_{\min}, \omega_{\max}]$ is the quasiparticle energy band,

$v = d\omega/dk$ is the quasiparticle group velocity, and the weight w accounts for the entropy contribution of a given pair.

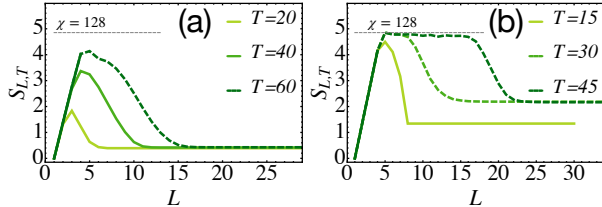


Figure 3. TE vs L , for several evolution times T (see legends), in the non-integrable KIC (3) with $g = 0.685$, $J = 0.31$, $h = 0.2$ (a) and $g = 0.724$, $J = 0.8$, $h = 0.647$ (b), calculated using MPS with $\chi = 128$. The hard upper bound $S_{\max} = \log \chi$ on TE is highlighted. Dashing indicates that data are not converged with χ .

We set $t = T/2$ for definiteness. Equation (1) implies that $S_{L,T}/T \equiv s(\xi)$ is a function of the geometric parameter $\xi = L/T$ only. Taking the limit $T \rightarrow \infty$ first, one obtains a strictly linear increase $S = v_{TE}L$, with $v_{TE} = 2 \int_{\omega_{\min}}^{\omega_{\max}} \frac{d\omega}{2\pi} \frac{w(\omega)}{v(\omega)}$ [33]. However, for finite ξ , the boundaries absorb slow quasiparticles with $v < 4\xi$, making the curve $s(\xi)$ bend down from the straight line $v_{TE}\xi$. When ξ exceeds $v_{\max}/4$, quasiparticles at all velocities are being absorbed, so s is now *decreasing* with ξ . Finally, approaching $v_{\max}/2$, only a vanishing fraction of fast quasiparticles avoid the boundaries. Thus, $s(\xi)$ has a barrier shape, sketched in Fig. 2(a). The infinite-system [$L > (v_{\max}/2)T$] TE entropy $S_{\infty,T}$ can be shown to saturate as $T \rightarrow \infty$ (*area-law*) in models with free ballistic quasiparticles [21]. The semiclassical formula (1) reproduces the extensive (*volume-law*) term of the asymptotic scaling $S \sim s(\xi) \cdot T + S_{\infty}$ as $T \rightarrow \infty$, which vanishes for $\xi \geq v_{\max}/2$.

To verify this TEB scenario, we computed $S_{L,T}$ in the transverse-field kicked Ising chain (KIC), described by the Floquet operator

$$U = e^{ig \sum_j X_j} e^{iJ \sum_j Z_j Z_{j+1}}, \quad (2)$$

with X_j, Z_j Pauli matrices acting on spin j . This model can be mapped onto a non-interacting fermionic chain. Figure 2(b) provides a comparison between the exact result, obtained using Grassmann path integral techniques [21], and the quasiparticle formula (1) with $w \equiv \text{const}$. The weight $w \equiv \log 2$ makes Eq. (1) exact at the self-dual points $|J| = |g| = \pi/4$ of the model [34], where $s(\xi) = \log 2 \min(\xi, 1/2 - \xi)$. The ansatz $w \equiv \text{const}$ captures the properties of TEB – including the location of its maximum – fairly well throughout the phase diagram [see Fig. 2(b)] [35].

We note that the simplifying assumptions of an infinite-temperature initial state and OBC are not crucial for the TEB phenomenology: As is clear

from the quasiparticle picture, neither the possible presence of counter-propagating entangled pairs at $\tau = 0$ [2], nor modified reflections at the edge of \mathcal{E} , affect the qualitative behavior [36]. We have explicitly checked this for different $\rho_{\mathcal{E}}$ and $|\mathcal{S}_{0,T}\rangle$ in the model (2) via exact computations and numerical simulations [cf. Ref. [25] and Fig. 4(c)].

As a next step, we demonstrate that TEB persists when integrability is broken, and quasiparticles acquire a finite lifetime and scatter, or may not even be well-defined. We consider the non-integrable KIC

$$U = e^{ig \sum_j X_j} e^{iJ \sum_j Z_j Z_{j+1}} e^{ih \sum_j Z_j} \quad (3)$$

initialized in an infinite-temperature state. We compute TEB with OBC using the MPS iterative algorithm detailed in Ref. [16], with a maximum bond dimension cutoff $\chi = 128$. In Fig. 3(a) we have considered a moderate breaking of integrability $h = 0.2$, for which quasiparticles are expected to have a finite lifetime. In Fig. 3(b), instead, we choose parameters $J, g, h = \mathcal{O}(1)$ found in Ref. [37] to give rise to random-matrix level statistics and to obey the eigenstate thermalization hypothesis. In this case the system is fully chaotic, without well-defined quasiparticles. Both these plots clearly show the existence of a high TEB. Approaching the peak at longest simulation times (dashed lines), the data become inaccurate, as the bond dimension is not sufficient to capture the massively entangled intermediate IMs.

Light-cone growth algorithm. We now describe a modified algorithm which combines space-time contractions to completely avoid TEB. This algorithm is illustrated in Fig. 4(a). The circuit defining the infinite-system IM is equivalent to a finite “triangular” network, obtained by erasing the unitary gates located beyond the light ray emanating backward in time from \mathcal{S} . By causality, such gates cannot produce any influence on \mathcal{S} – a manifestation of the strict light-cone effect of circuit dynamics. We now contract this reduced network in the space direction. At the n -th step, the computation produces the *infinite-system* IM corresponding to evolution time $T = n$, $|\mathcal{S}_{2n,n}\rangle \equiv |\mathcal{S}_{\infty,n}\rangle$. The following one $T = n + 1$ is obtained by applying \tilde{T}_{n+1} to the IM $|\mathcal{S}_{2n,n}\rangle \otimes |\mathbb{1}_2\rangle \otimes \frac{1}{2}|\mathbb{1}_2\rangle$, as shown in Fig. 4(b).

For translationally invariant chains, this algorithm circumvents TEB, since $S_{\infty,T}$ scales monotonically with T . This fact is intuitively true, as all the information encoded in $|\mathcal{S}_{\infty,T}\rangle$ is strictly included in $|\mathcal{S}_{\infty,T+t}\rangle$. Monotonicity, i.e., $S_{\infty,T} \leq S_{\infty,T+t}$, can be proven by noting that $|\mathcal{S}_{\infty,T}\rangle$ is obtained from $|\mathcal{S}_{\infty,T+t}\rangle$ by projecting its last t pairs of legs onto $\bigotimes_{\tau=T+1}^{T+t} \frac{1}{2}(|\mathbb{1}\rangle \otimes |\mathbb{1}\rangle)$, which follows from erasing the whole last t layer of gates using unitarity [cf.

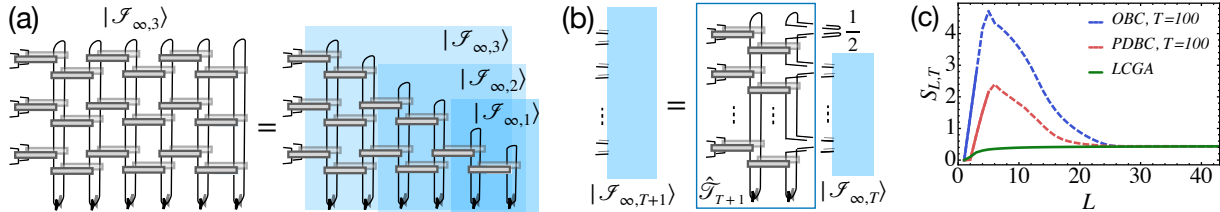


Figure 4. (a): Intermediate LCGA steps produce the sequence of bulk IMs for increasing T (blue-shaded boxes). (b): Iterative LCGA step. (c): Comparison of TE vs iterative step of $\hat{\mathcal{T}}$ -iterations with OBC, PDBC and LCGA.

Fig. 4(a)]. By construction, entanglement is strictly non-increasing under this local projection operation, for arbitrary bipartition cuts.

In Fig. 4(c) we report the results of three different computations of the bulk IM for the same model and parameters as in Fig. 3(a): (i) iterations from OBC, (ii) iterations from “perfect-dephaser” boundary condition (PDBC), i.e., $|\mathcal{S}_{0,T}\rangle = \bigotimes_{\tau=1}^T \frac{1}{2}|\mathbb{1}\rangle \otimes |\mathbb{1}\rangle$ (cf. Refs. [16, 17]), (iii) LCGA. For each of them, we computed $S_{L,T}$ as a function of L viewed as the iteration counter. The PDBC IM shows a partially mitigated TEB, since it represents the IM of a maximally chaotic circuit [16], closer to the bulk IM of the chaotic model under consideration compared to the OBC IM (i). However, this $|\mathcal{S}_{0,T}\rangle$ also generates boundary “reflections” of quantum information, giving rise to an extensive TEB. Most importantly, TEB is fully circumvented by LCGA.

Outlook. The IM approach offers an alternative route to the evolution of local observables, relevant for studying thermalization and transport in strongly interacting quantum many-body systems. Unlike previous proposals [5–13], this approach does not involve *ad hoc* truncation of non-local quantum information, and possibly circumvents the exponential wall of quantum many-body dynamics whenever the scaling of TE entropy with evolution time is sublinear – which has been demonstrated in several physically distinct regimes [17, 21–25, 28]. The generic greater efficiency of the “transverse contraction and folding” MPS algorithm was empirically observed in early applications (see Refs. [18, 19] and [1]). The findings of this work lay a firm physical basis for the origin of this efficiency, at the same time establishing a more direct way to exploit it.

Furthermore, this work reveals a novel aspect of space-time duality [31, 34, 38–44]: Keldysh boundary conditions play a crucial role for the TEB effect, which is absent in the pure-state spacetime-dual evolution discussed in the context of measurement-induced entanglement transitions [40, 41]. This will hopefully stimulate further research in this direction,

e.g., concerning a comprehensive quantitative understanding of the quasiparticle picture of TE scaling with general boundaries. Another interesting direction is to develop an efficient version of the LCGA for Hamiltonian dynamics, where the unphysical light velocity of the Trotterized circuit $v_{lc} = 2/\Delta t \gg 1$ is to be replaced by the physical Lieb-Robinson velocity $v_{max} = \mathcal{O}(1)$. Such an algorithm, in particular, is expected to be suitable for studying transport phenomena in correlated systems. Finally, an important open question – which will be addressed elsewhere – is to clarify the general relation between TEB and real-space entanglement barriers [45–47].

Acknowledgments. This work was supported by the Swiss National Science Foundation and by the European Research Council (ERC) under the European Union’s Horizon 2020 research and innovation programme (grant agreement No. 864597).

-
- [1] U. Schollwöck, *Annals of physics* **326**, 96 (2011).
 - [2] P. Calabrese and J. Cardy, *Journal of Statistical Mechanics: Theory and Experiment* **2005**, P04010 (2005).
 - [3] H. Kim and D. A. Huse, *Phys. Rev. Lett.* **111**, 127205 (2013).
 - [4] A. Nahum, J. Ruhman, S. Vijay, and J. Haah, *Phys. Rev. X* **7**, 031016 (2017).
 - [5] E. Leviatan, F. Pollmann, J. H. Bardarson, D. A. Huse, and E. Altman, *arXiv preprint arXiv:1702.08894* (2017).
 - [6] B. Kloss, Y. B. Lev, and D. Reichman, *Phys. Rev. B* **97**, 024307 (2018).
 - [7] C. D. White, M. Zaletel, R. S. K. Mong, and G. Refael, *Phys. Rev. B* **97**, 035127 (2018).
 - [8] J. Surace, M. Piani, and L. Tagliacozzo, *Phys. Rev. B* **99**, 235115 (2019).
 - [9] B. Ye, F. Machado, C. D. White, R. S. K. Mong, and N. Y. Yao, *Phys. Rev. Lett.* **125**, 030601 (2020).
 - [10] C. Krumnow, J. Eisert, and Ó. Legeza, *arXiv preprint arXiv:1904.11999* (2019).
 - [11] T. Rakovszky, C. von Keyserlingk, and F. Pollmann, *arXiv preprint arXiv:2004.05177* (2020).
 - [12] C. Karrasch, J. H. Bardarson, and J. E. Moore,

- New Journal of Physics **15**, 083031 (2013).
- [13] J. Hauschild, E. Leviatan, J. H. Bardarson, E. Altman, M. P. Zaletel, and F. Pollmann, *Phys. Rev. B* **98**, 235163 (2018).
- [14] R. Feynman and F. Vernon, *Annals of Physics* **24**, 118 (1963).
- [15] A. J. Leggett, S. Chakravarty, A. T. Dorsey, M. P. A. Fisher, A. Garg, and W. Zwerger, *Rev. Mod. Phys.* **59**, 1 (1987).
- [16] A. Lerose, M. Sonner, and D. A. Abanin, *Phys. Rev. X* **11**, 021040 (2021).
- [17] M. Sonner, A. Lerose, and D. A. Abanin, *Annals of Physics* **435**, 168677 (2021), special issue on Philip W. Anderson.
- [18] M. C. Bañuls, M. B. Hastings, F. Verstraete, and J. I. Cirac, *Phys. Rev. Lett.* **102**, 240603 (2009).
- [19] A. Müller-Hermes, J. I. Cirac, and M. C. Bañuls, *New Journal of Physics* **14**, 075003 (2012).
- [20] E. Ye and G. Kin-Lic Chan, arXiv e-prints, arXiv:2101.05466 (2021), arXiv:2101.05466 [quant-ph].
- [21] A. Lerose, M. Sonner, and D. A. Abanin, *Phys. Rev. B* **104**, 035137 (2021).
- [22] L. Piroli, B. Bertini, J. I. Cirac, and T. c. v. Prosen, *Phys. Rev. B* **101**, 094304 (2020).
- [23] K. Klobas, B. Bertini, and L. Piroli, arXiv e-prints, arXiv:2012.12256 (2020), arXiv:2012.12256 [cond-mat.stat-mech].
- [24] K. Klobas and B. Bertini, *SciPost Phys.* **11**, 106 (2021).
- [25] G. Giudice, G. Giudici, M. Sonner, J. Thoenniss, A. Lerose, D. A. Abanin, and L. Piroli, arXiv preprint arXiv:2112.14264 (2021).
- [26] G. Vidal, *Phys. Rev. Lett.* **93**, 040502 (2004).
- [27] I. A. Luchnikov, S. V. Vintskevich, H. Ouerdane, and S. N. Filippov, *Phys. Rev. Lett.* **122**, 160401 (2019).
- [28] M. Sonner, A. Lerose, and D. A. Abanin, arXiv e-prints, arXiv:2012.00777 (2020), arXiv:2012.00777 [cond-mat.dis-nn].
- [29] Recall that we work with the Keldysh path integral, and therefore each trajectory has a forward and backward part.
- [30] E. H. Lieb and D. Robinson, *Commun. Math. Phys.* **28**, 251 (1972).
- [31] B. Bertini, P. Kos, and T. c. v. Prosen, *Phys. Rev. Lett.* **123**, 210601 (2019).
- [32] With a reflection coefficient related to the cross section of production.
- [33] Note that $v(\omega) \sim \sqrt{\omega - \omega_{\min}}$ or $\sqrt{\omega_{\max} - \omega}$ at the quasienergy band edges, and the entropy contribution of pairs is bounded as $w(\omega) \leq 2 \log 2$ (the factor 2 accounts for the two branches of the Keldysh contour). Thus, the integral that defines v_{TE} is convergent.
- [34] M. Akila, D. Waltner, B. Gutkin, and T. Guhr, *Journal of Physics A: Mathematical and Theoretical* **49**, 375101 (2016).
- [35] We note that the exact entropy function $w(\omega)$ cannot be expressed in terms of the microscopic data of the model by straightforwardly generalizing the standard arguments valid for unitary dynamics [48]: the non-unitary generator $\hat{\mathcal{T}}$ is non-diagonalizable [16], which makes the formulation of a generalized Gibbs ensemble for the dual dynamics *a priori* unclear. It could presumably be obtained by generalizing the calculation of Ref. [49] to non-unitary evolution.
- [36] Here we are considering initial states with a pair structure of quasiparticles, as usually arising from global quenches [2]. We note that fine-tuned examples are known for which this is not the case [50, 51]. In this case, a different behavior could be envisaged.
- [37] H. Kim, T. N. Ikeda, and D. A. Huse, *Phys. Rev. E* **90**, 052105 (2014).
- [38] B. Bertini, P. Kos, and T. c. v. Prosen, *Phys. Rev. Lett.* **121**, 264101 (2018).
- [39] M. Ippoliti and V. Khemani, *Phys. Rev. Lett.* **126**, 060501 (2021).
- [40] T.-C. Lu and T. Grover, *PRX Quantum* **2**, 040319 (2021).
- [41] M. Ippoliti, T. Rakovszky, and V. Khemani, arXiv preprint arXiv:2103.06873 (2021).
- [42] A. Chan, A. De Luca, and J. T. Chalker, *Phys. Rev. Research* **3**, 023118 (2021).
- [43] S. J. Garratt and J. T. Chalker, *Phys. Rev. X* **11**, 021051 (2021).
- [44] S. J. Garratt and J. T. Chalker, *Phys. Rev. Lett.* **127**, 026802 (2021).
- [45] J. Dubail, *Journal of Physics A: Mathematical and Theoretical* **50**, 234001 (2017).
- [46] H. Wang and T. Zhou, *Journal of High Energy Physics* **2019**, 1 (2019).
- [47] I. Reid and B. Bertini, *Phys. Rev. B* **104**, 014301 (2021).
- [48] V. Alba and P. Calabrese, *Proceedings of the National Academy of Sciences* **114**, 7947 (2017), <https://www.pnas.org/content/114/30/7947.full.pdf>.
- [49] M. Fagotti and P. Calabrese, *Phys. Rev. A* **78**, 010306 (2008).
- [50] B. Bertini, E. Tartaglia, and P. Calabrese, *J. Stat. Mech.* **2018**, 063104 (2018).
- [51] A. Bastianello and P. Calabrese, *SciPost Phys.* **5**, 33 (2018).